

# Reliability and Cost Optimization of Multi-input Bidirectional DC/DC Converter Implemented in Renewable Sources

Farhad Abbasi Aghdam Meinagh<sup>1\*</sup>, Mehdi Abapour<sup>2</sup>

1- Department of Electrical & Computer Engineering, Faculty of Electrical Engineering, University of Tabriz, Tabriz, Iran.  
Email: Mehdi.abapour@gmail.com (Corresponding author)

2- Department of Electrical & Computer Engineering, Faculty of Electrical Engineering, University of Tabriz, Tabriz, Iran.  
Email: farhadabbasi2015@gmail.com

Received: February 2018

Revised: May 2018

Accepted: July 2018

## ABSTRACT:

Due to the increasing use of renewable energy sources, employing a DC/DC converter as the interface is proliferated. Among various DC/DC topologies, utilizing multi-input converters due to higher reliability and flexibility is more widespread. This paper evaluates the reliability of the multi-input DC/DC converter, besides carrying out cost calculation to achieve a cost-effective and reliable converter. Furthermore, diagrams of various reliability factors versus the converter's branches are demonstrated based on mathematical equations and simulation values for both of parallel and standby redundant modes in order to reach an optimal number of branches in each mode. The results show that the optimal number of branches in terms of reliability or cost factor is different and can vary based on some parameters like output power or component's type.

**KEYWORDS:** Multi-input DC/DC Converter, Reliability Calculation, Cost Optimization, Renewable Energy.

## 1. INTRODUCTION

Recent advancements in renewable energy sources such as fuel cell (FC) and photovoltaic panels cause new challenges in power converters designing. Electricity network, in the future, needs an interface converter which is able to transform different renewable energy sources to electricity, simultaneously. In order to achieve this aim, the multi-input power converter is required. An ideal multi-input power converter can be connected to each renewable energy source and take its advantages. Moreover, the existence of diverse energy sources in multi-input converter increases the system's reliability [1]. The reliability of each exploited component in power electronic converters has a fundamental role in correct operation of the converter and, eventually the primary system. Experience shows that electrolyte capacitors and power switches like IGBT and MOSFET are the most vulnerable components in power electronic converters [2].

[3] is offering an industry-based reliability survey of power electronic converters. Reliability prediction and high-power switches modelling like MOSFET and IGBT are carried out in [4], where in [5], a solution to improve the reliability of DC-link capacitors is presented. Furthermore, reliability calculation for multi-level converters is performed in [6] and also, the effect

of series and shunt redundancy on Power Semiconductor Reliability is presented in [7].

The main step of achieving high-reliability converters is designing a proper topology [8]. Various methods can be exploited to increase the reliability of the system; the first approach is estimation more than nominal values in power electronic converter components designing. The second method is using redundant branches. The redundant branch can operate instead of failed one, during system fault, to prevent any disruption in system's operation. The final solution is collecting information about the operating environment and failure rate which can be utilized in redesigning of the converter. The first two approaches enlarge the cost of the converter, while the third one demands information about many similar converters.

In a recent work [9], by using redundant branches, i.e. the second method, the reliability of the system is increased. Moreover, the redundant branches have several kinds and are used in power electronic converters such as inverters [10], multi-level converters [11], motor drives [12], DC/DC converters [13], and power factor correction (PFC) rectifiers [14]. These topologies usually act as a set of different equipment and a subset of the main circuit as redundant. For instance, a leg is added to the three-leg multi-level clamped inverter in

[15]. In [16], in addition to calculation of reliability and cost for the inverter using mathematical functions, the optimum number of redundant inverters is computed.

The presence of redundant branches both increase the reliability of the converter and diminish repair and replacement costs in case of failure. Despite various advantages, increasing the number of redundant branches will multiply the primitive cost which is not desirable for consumers. Research results show that after growing the number of redundant branches to a particular level, the system reliability does not change a lot [17].

In this paper, in order to increase the reliability, redundant branches are added to the DC/DC converter which can operate in both parallel and standby modes. Then, corresponded calculations are also made separately to specify the optimum number of branches for achieving the maximum reliability. Besides calculation of the reliability, installation, implementation, losses and maintenance cost functions of the converter are calculated. Thus, by calculation of the optimum number of branches, it is desired to achieve a cost-effective converter with high reliability.

**2. PARAMETERS EFFECT ON FAILURE RATE**

Fig. 1 depicts a conventional bidirectional buck-boost DC/DC converter including an input inductor, an output capacitor, two anti-parallel diodes and two switches. In order to calculate the converter reliability, the failure rate of each element must be computed. To calculate the components reliability, the relations in [18] are used.

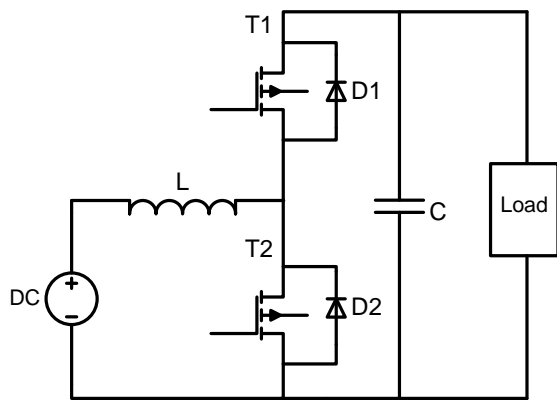


**Fig. 1.** The single-input bidirectional buck-boost DC/DC converter.

Fig. 2 shows a bidirectional dc/dc converter with  $M + N$  input branches in which  $M$  branches can provide maximum required power and the next  $N$  branches are redundant for the main branches and used to increase the converter reliability. It is assumed that all branches in Fig. 2 are identical and are in the parallel redundant mode. Thus, the same current flows through each of

them, which is reciprocal to the number of used branches. In the redundant standby mode, the same current flows through only main branches.

According to [18], the net failure rate of the single-input bidirectional buck-boost DC/DC converter in Fig. 1 is dependent on several parameters, which are demonstrated in Table 1. In Table 1, general relations of the bidirectional buck-boost DC/DC converter components failure rate are illustrated, which are in 1/million hour.

In Tables 2 and 3, the failure rate is expressed in terms of more tangible parameters such as duty cycle, year of manufacture and temperature.

**Table 1.** The bidirectional buck-boost dc/dc converters parametric failure rate.

Elements	Failure Rate Relation
MOSFET	$\pi_G(\lambda_{OB}\pi_{DCO}\pi_{TO}\pi_S + \lambda_{EB}\pi_{DCN}\pi_{TE} + \lambda_{TCB}\pi_{CR}\pi_{DT}) + \lambda_{SIB}\pi_{SJD} + \lambda_{IND}$
Diode	$\pi_G(\lambda_{OB}\pi_{DCO}\pi_{TO}\pi_S + \lambda_{EB}\pi_{DCN}\pi_{TE} + \lambda_{TCB}\pi_{CR}\pi_{DT}) + \lambda_{SIB}\pi_{SJD} + \lambda_{IND}$
Inductor	$\pi_G(\lambda_{OB}\pi_{DCO}\pi_{TO} + \lambda_{EB}\pi_{DCN}\pi_{TE} + \lambda_{TCB}\pi_{CR}\pi_{DT}) + \lambda_{IND}$
Capacitor	$\pi_G\pi_C(\lambda_{OB}\pi_{DCO}\pi_{TO}\pi_S + \lambda_{EB}\pi_{DCN}\pi_{TE} + \lambda_{TCB}\pi_{CR}\pi_{DT}) + \lambda_{SIB}\pi_{SJD} + \lambda_{IND}$

**Table 2.** The equivalent common parameters in switch, diode, inductor and capacitor.

Common Parameters	$\pi_G$	$\pi_{DCO}$	$\pi_{DCN}$	$\pi_{CR}$
Equivalent Form	$e^{(-\beta(Y-1993))}$	$\frac{DC}{DC_{top}}$	$\frac{1-DC}{DC_{nonop}}$	$\frac{CR}{CR_1}$

Temperature is an important factor in systems reliability. In Table 3, four determining parameters which are related to temperature are introduced. All parameters presented in Tables 2 and 3 are constant and their values can be obtained from [18] in terms of environmental condition, manufacturing year and operating condition except temperature factors dependent on  $T_R$ .

**3. EFFECT OF  $T_R$  ON FAILURE RATE**

Junction temperature  $T_j$  is a variable quantity, in which failure rate  $\lambda$  is dependent to that, and defined as:

$$T_j = T_{AO} + T_R \tag{1}$$

As stated in nomenclature,  $T_{AO}$  is ambient temperature during operation and  $T_R$  is junction

temperature increasing independent of environmental conditions, which is defined as:

$$T_R = \theta_{jA} \times P_D \tag{2}$$

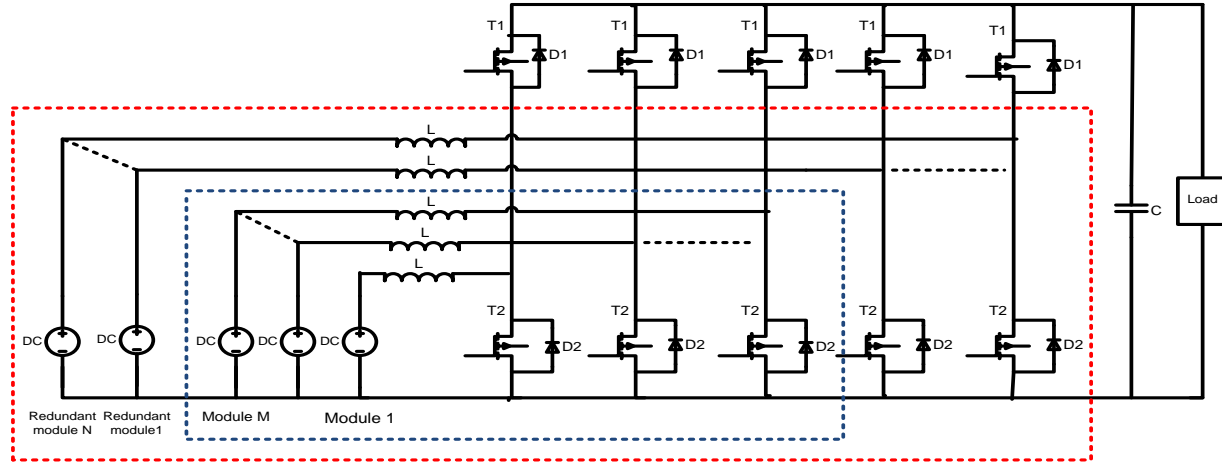


Fig. 2. The general form of bidirectional buck-boost DC/DC converter with  $M$  main parallel and  $N$  redundant parallel branches.

Table 3. Temperature coefficient in failure rate calculation.

	Failure Rate Multiplier for Temperature, Operating	Failure Rate Multiplier, Temperature – Environment	Failure Rate Multiplier, Delta Temperature	Failure Rate Multiplier, Solder Joint Delta Temperature
Capacitor	$\pi_{TO} = e^{\left(\frac{-Ea_{op}}{0.00008617} \left(\frac{1}{T_{AO}+273} - \frac{1}{298}\right)\right)}$	$\pi_{TE} = e^{\left(\frac{-Ea_{mop}}{0.00008617} \left(\frac{1}{T_{AE}+273} - \frac{1}{298}\right)\right)}$	$\pi_{DT} = \left(\frac{T_{AO} - T_{AE}}{DT_1}\right)^2$	$\pi_{SIDT} = \left(\frac{T_{AO} - T_{AE}}{44}\right)^{2.26}$
Diode	$\pi_{TO} = e^{\left(\frac{-Ea_{op}}{0.00008617} \left(\frac{1}{T_{AO}+T_R+273} - \frac{1}{298}\right)\right)}$	$\pi_{TE} = e^{\left(\frac{-Ea_{mop}}{0.00008617} \left(\frac{1}{T_{AE}+273} - \frac{1}{298}\right)\right)}$	$\pi_{DT} = \left(\frac{T_{AO} + T_R - T_{AE}}{DT_1 = 80}\right)^2$	$\pi_{SIDT} = \left(\frac{T_{AO} + T_R - T_{AE}}{44}\right)^{2.26}$
Inductor	$\pi_{TO} = e^{\left(\frac{-Ea_{op}}{0.00008617} \left(\frac{1}{T_{AO}+T_R+273} - \frac{1}{298}\right)\right)}$	$\pi_{TE} = e^{\left(\frac{-Ea_{mop}}{0.00008617} \left(\frac{1}{T_{AE}+273} - \frac{1}{298}\right)\right)}$	$\pi_{DT} = \left(\frac{T_{AO} + T_R - T_{AE}}{DT_1 = 8.94}\right)^2$	Doesn't exist
MOSFET	$\pi_{TO} = e^{\left(\frac{-Ea_{op}}{0.00008617} \left(\frac{1}{T_{AO}+T_R+273} - \frac{1}{298}\right)\right)}$	$\pi_{TE} = e^{\left(\frac{-Ea_{mop}}{0.00008617} \left(\frac{1}{T_{AE}+273} - \frac{1}{298}\right)\right)}$	$\pi_{DT} = \left(\frac{T_{AO} + T_R - T_{AE}}{DT_1 = 80}\right)^2$	$\pi_{SIDT} = \left(\frac{T_{AO} + T_R - T_{AE}}{44}\right)^{2.26}$

In the above equation,  $\theta_{jA}$  is thermal impedance between the connection point and surrounding environment and  $P_D$  is dissipated power in elements, which is demonstrated in Table 4. Integrating these relations over duty cycle, dissipated power can be obtained. As can be seen from Table 4, resistance and internal voltage drop of components are dependent on their raw material used during the manufacturing process and are constant. In other words, the only variable changes dissipated power,  $P_D$  is the current flow through the component.

With multiplying mentioned current,  $P_D$ ,  $T_r$  and  $\lambda$  are also increasing according to (2) and relations in Tables 1, 3 and 4.

Table 4. The equivalent circuit and calculation of the circuit components losses [18]

	Equivalent Circuit	Power Loss
MOSFET	$V_T$ $R_{DS}$ 	$P_D = i_s^2(t)R_{DS(on)} + i_s(t)V_T$
Diode	$V_F$ $r_D$ 	$P_D = i_D^2(t)r_{D(on)} + i_D(t)V_F$
Inductor	$r_{esr}$ 	$P_D = r_{esr}i_L^2(t)$

Omitting switching losses, following equations for the bidirectional DC/DC converter components power losses in a duty cycle can be obtained. For switches power losses, have:

$$\begin{aligned}
 P_{D,switches} &= P_{D,T1} + P_{D,T2} \\
 &= \frac{1}{T} \left( \int_0^T (V_{T,T1} + R_{DS(on),T1} i_{s,T1}(t)) i_{s,T1}(t) dt \right. \\
 &\quad \left. + \int_0^T (V_{T,T2} + R_{DS(on),T2} i_{s,T2}(t)) i_{s,T2}(t) dt \right) \quad (3) \\
 &= D(V_{T,T1} + R_{DS(on),T1} i_{s,T1}(t)) i_{s,T1}(t) \\
 &\quad + (1-D)(V_{T,T2} + R_{DS(on),T2} i_{s,T2}(t)) i_{s,T2}(t)
 \end{aligned}$$

Where,  $T$  is the switching period in above equation. Since both switches are identical, and circuit topology is symmetrical, have:

$$P_{D,switches} = (V_T + R_{DS(on)} i_s(t)) i_s(t) \quad (4)$$

Diodes power losses relations are similar to the switches losses and as a consequence, for the depicted converter in Fig. 1, the diodes power losses are:

$$P_{D,Diodes} = (V_F + r_{D(on)} i_D(t)) i_D(t) \quad (5)$$

Due to bulky input inductor in Fig. 1, the current flowing through the inductor is assumed to be constant i.e.  $i_L(t) \approx I_L$ .

The diodes and switches power losses can be acquired by substituting the simulation current values flowing through each of the components in (4), (5), where the simulation values will be obtained in next chapter.

#### 4. QUANTITATIVE CALCULATION OF THE SINGLE-INPUT BIDIRECTIONAL BUCK-BOOST DC-DC CONVERTER RELIABILITY

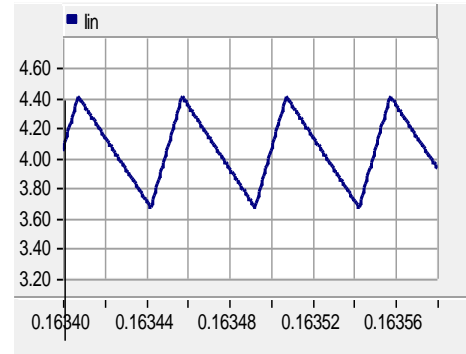
##### 4.1. Simulation Results

The bidirectional buck-boost DC/DC converter shown in Fig. 1 is simulated in PSCAD EMTDC environment using values in Table 5 to observe flowing currents and, as a result, each component losses.

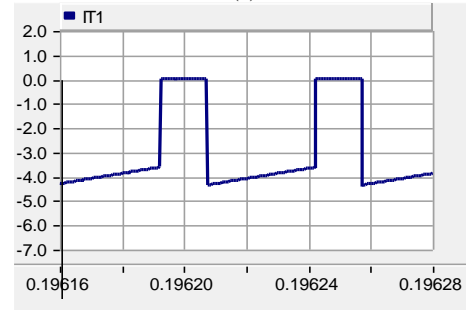
**Table 5.** The parameters of bidirectional buck-boost dc/dc converter shown in Fig. 1.

Circuit Parameters	Value
Input voltage	$100V_{DC}$
Output voltage	$140V_{DC}$
Switching Frequency	$20kHz$
MOSFET	$IRF740MOSFET, R_{on,mosfet} = 0.1\Omega$
Diode	$MUR1560Diode, R_{on,Diode} = 0.1\Omega$
The internal resistance of the input inductor	$0.1\Omega$
Input inductor	$2mH$
Output capacitor	$400\mu F$
Duty cycle	$0.3$
Rated power	$400W$

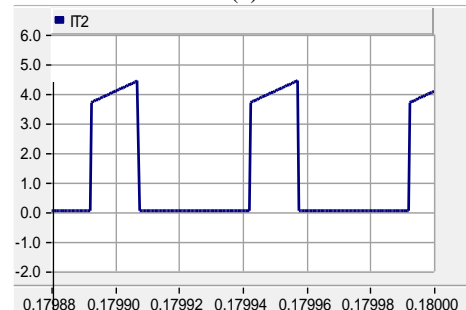
Flowing current of each component, in addition to the output voltage of bidirectional buck-boost DC/DC converter is shown in Fig. 3. Power losses of the circuit components can be calculated by using the flowing current through the elements shown in Fig. 3.



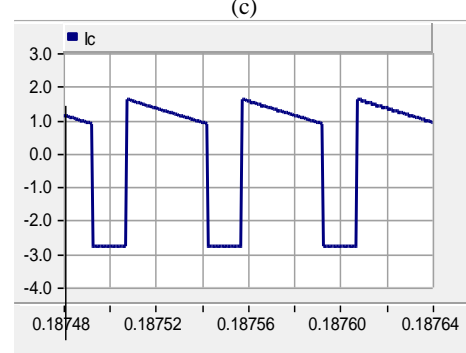
(a)



(b)



(c)



(d)

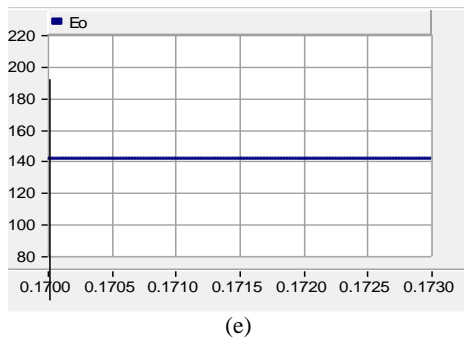


**Fig. 3.** The Simulation results of bidirectional buck-boost DC/DC converter; (a) input current or flowing current through the  $L$  inductor, (b) flowing current through the  $T_1$  switch, (c) flowing current through the  $T_2$  switch, (d) flowing current through the output filter capacitor, (e) output voltage.

**4.2. Quantitative Reliability Calculation**

Given to the relationships in Tables 1, 2, 3, 4, values obtained in [18], (4) and (5) and flowing current through the elements shown in Fig.3, the failure rates of the components in Fig. 1, are listed in Table 6. According to Table 6, the failure rate of the inductor is very low which indicates that the inductor is the last element which fails in an electrical converter. The total failure rate for the converter in Fig. 1 is as follows:

$$\lambda_{total(\sin gle)} = 2(\lambda_1 + \lambda_2) + \lambda_3 + \lambda_4 = 1.0512 / \text{million hours} \quad (6)$$

$$MTBF_{\sin gle} = \frac{1}{\lambda_{total}} = 0.9513 \text{million hours} \quad (7)$$

The repair rate for this converter is supposed as 24 days and can be written as follows:

$$\mu_{total(\sin gle)} = 1736.111 / \text{million hours} \quad (8)$$

$$A_{\sin gle} = \frac{\mu_{total}}{\mu_{total} + \lambda_{total}} = 0.9994 \quad (9)$$

**Table 6.** The failure rate of the components in Fig. 1.

COMPONENT NAME	$\lambda$ (per million hours)
MOSFET	$\lambda_1 = 0.296$
Diode	$\lambda_2 = 0.0243$
Inductor	$\lambda_3 = 14.2 \times 10^{-6}$
Capacitor	$\lambda_4 = 0.41$

**5. QUANTITIVE CALCULATION OF THE BIDIRECTIONAL BUCK-BOOST CONVERTER RELIABILITY WITH  $M$  AND  $N$  REDUNDANT BRANCHES**

As can be seen in Fig. 2, efficient performance of the converter demands proper operation of all the main branches, while the redundant branches are used only for increasing the reliability. Also, it is assumed that the

branches reliability is independent of each other and, in standby mode, a spare switch is connected in series with the input inductor in each redundant branch and it conducts when one of the main branches is out of service.

The converter reliability with  $M + N$  branches in parallel operating mode can be calculated as:

$$\lambda_{M+N,Parallel} = \frac{1}{MTBF_{M+N}} = \frac{1}{\frac{1}{\sum_{i=M}^{M+N} \frac{1}{\lambda_{total(\sin gle)}^i}}} \quad (10)$$

$$A_{M+N,Parallel} = \sum_{i=M}^{M+N} \binom{M+N}{i} A_{\sin gle}^i (1 - A_{\sin gle})^{M+N-i} \quad (11)$$

As stated above, in standby mode, a switch is added to each redundant branch, which is included in the failure rate calculation. Equations (12)-(14), for standby mode, are calculated as below:

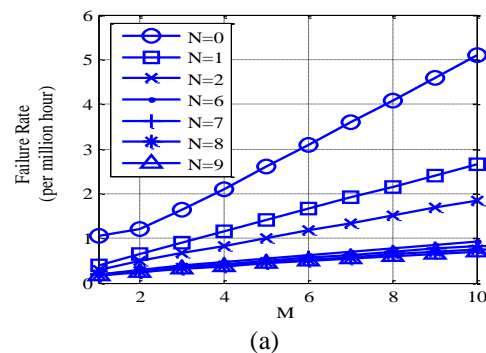
$$\lambda'_{total(\sin gle)} = 3\lambda_1 + 2\lambda_2 + \lambda_3 + \lambda_4 = 1.3472 / \text{million hours} \quad (12)$$

$$\lambda'_{M+N,S} = \frac{1}{MTBF'_{M+N}} = \frac{1}{\frac{1}{\sum_{i=M}^{M+N} \frac{1}{\lambda'_{total(\sin gle)}^i}}} \quad (13)$$

$$A'_{M+N,S} = \sum_{i=M}^{M+N} \binom{M+N}{i} A'_{\sin gle}{}^i (1 - A'_{\sin gle})^{M+N-i} \quad (14)$$

$\lambda'_{total(\sin gle)}$ ,  $\lambda'_{M+N,S}$  and  $A'_{M+N,S}$  are related to redundant standby mode. Figs. 4 and 5 illustrate the failure rate and availability diagrams in terms of  $M$  and  $N$  variations.

It can be observed from Fig. 4 that generally, with increasing number of main branches  $M$ , the failure rate multiplies and with increasing number of redundant branches  $N$ , either in a parallel or in a standby mode, the failure rate of the system diminishes. In addition, it can be seen from Fig. 4(a), when the number of parallel redundant branches is more than six, the failure rate does not change, especially in a lower number of main branches. Thus, adding more than 6 redundant branches is not economical.



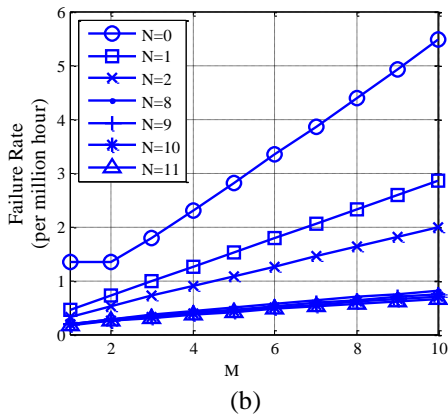


**Fig. 4.** The converter failure rate diagram with  $N$  redundant branches in terms of  $M$  and  $N$  variations; (a) parallel redundant; (b) standby redundant.

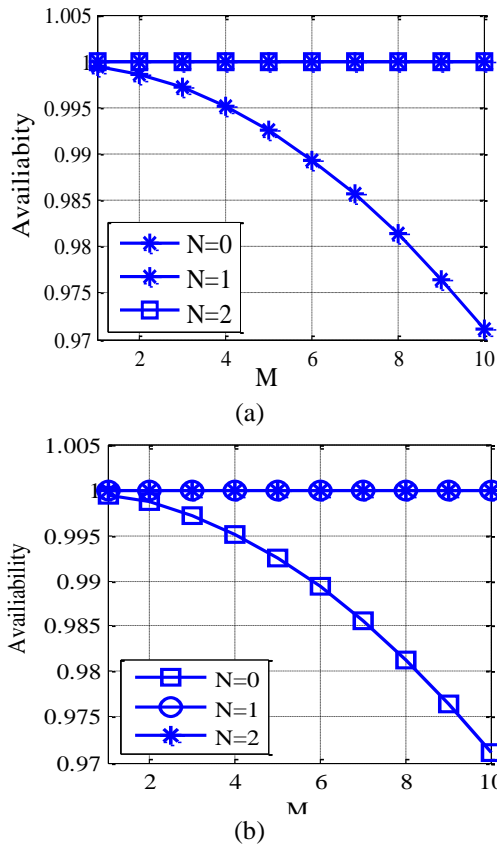


**Fig. 5.** The converter availability variation diagram with  $N$  redundant branches in terms of  $M$  and  $N$  variations; (a) parallel redundant; (b) standby redundant

In redundant standby mode, which its failure rate diagram is shown in Fig. 4(b), when  $N \geq 8$ , the failure rate does not change a lot. Thus, if  $N = 8$  the converter will be cost-effective and high reliable.

It can be observed from Fig. 5, with adding a branch either in parallel or standby mode to the main branches, the system's availability becomes almost one. On the

contrary, in a system without redundant branches, with increasing the number of  $M$ , the system availability decreases. For better clarification, the failure rate and availability values for branches including two main and one parallel redundant branches are calculated as follows:

$$\lambda_{total(2+1)} = 0.6518 / \text{million hours} \quad (15)$$

$$MTBF_{(2+1)} = \frac{1}{\lambda_{total(2+1)}} = 1.53 \text{million hours} \quad (16)$$

$$\mu_{total(2+1)} = 1736.111 / \text{million hours} \quad (17)$$

$$A_{(2+1)} = \frac{\mu_{(2+1)}}{\mu_{(2+1)} + \lambda_{total(2+1)}} = 1 \quad (18)$$

## 6. OPTIMIZATION OF BRANCHES BASED ON COST CALCULATION

Related costs of each system are depended on system's performance, sensitivity and components. The most significant and common costs exist for the power electronic converters which are: (a) Installation cost, (b) Cost of losses, (c) Performance and maintenance cost including; Scheduled maintenance, Unscheduled maintenance and System failure costs.

For some relations and costs used in this section, equations presented in [19] are employed. The calculation of cost is carried out for 5 years and the bidirectional buck-boost converter price is assumed 0.2\$/W, the converter rated power is  $P_o = 3kW$  and the efficiency is 90%. The installation cost for the P kW parallel buck-boost converter with  $M$  main and  $N$  redundant branches is as below:

$$C_{install} = 200 \times P \times (1 + \frac{N}{M}) + 100(M + N) \quad (19)$$

The scheduled maintenance cost is, typically, 5%-6% of the installation cost. Thus, the scheduled maintenance cost for 5 years is as follows:

$$C_{O\&M,s} = C_{install} \times 5\% \times 5 \quad (20)$$

The unscheduled maintenance cost over 5 years is as below:

$$C_{O\&M,u} = \lambda_{M+N} \times 5 \times (C_{rep} + C_l \times MTTR) \quad (21)$$

$$C_{rep} = 200 \times P \times \frac{1}{M} \quad (22)$$

$C_{rep}$  is the component replacement cost. Worker wages and the trip cost for each fail  $C_l$  are about

300\$/day per kW [19]. Substituting (10) and (22) in (21) have:

$$C_{O\&M,u} = \frac{1}{\frac{1}{\lambda_{total(sin\ gl e)}} \sum_{i=M}^{M+N} \frac{1}{i}} \times 5 \times (200 \times P \times \frac{1}{M} + C_l \times \frac{1}{\mu}) \quad (23)$$

The cost related to out of service system is depended on the system's availability. This cost for each day is about 50\$. Thus, during 5 years, the total is:

$$\begin{aligned} C_{down} &= 5 \times (1 - A_{M+N}) \times 50 \times 365 \\ &= (1 - \sum_{i=M}^{M+N} \binom{M+N}{i} A_{sin\ gl e}^i (1 - A_{sin\ gl e})^{M+N-i}) \times 91250 \end{aligned} \quad (24)$$

The cost of loss is assumed 10c/kWh. Therefore, for a 5-years period, the total cost of loss is:

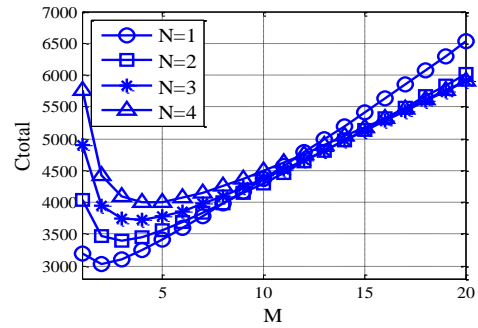
$$C_{loss} = (1 - \eta) \times P \times 0.1 \times 24 \times 365 \times 5 = (1 - \eta) \times P \times 4380 \quad (25)$$

The total cost is equal to the sum of the aforementioned costs, which can be written as follows:

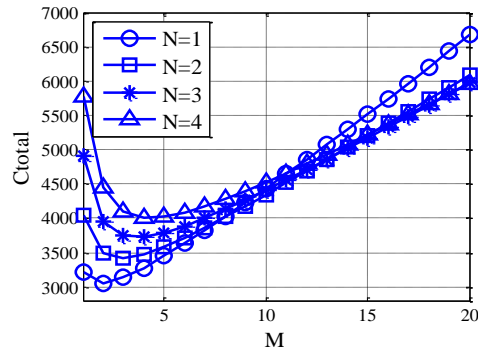
$$\begin{aligned} C_{total}(M,N) &= C_{install} + C_{O\&M,s} + C_{O\&M,u} + C_{down} + C_{loss} \\ &= 1.25 \times (200 \times P \times (1 + \frac{N}{M}) + 100 \times (M + N)) \\ &\quad + \frac{1}{\frac{1}{\lambda_{total(sin\ gl e)}} \sum_{i=M}^{M+N} \frac{1}{i}} \times 5 \times (200 \times P \times \frac{1}{M} + C_l \times \frac{1}{\mu}) \\ &\quad + (1 - \sum_{i=M}^{M+N} \binom{M+N}{i} A_{sin\ gl e}^i (1 - A_{sin\ gl e})^{M+N-i}) \\ &\quad \times 91250 + (1 - \eta) \times P \times 4380 \end{aligned} \quad (26)$$

Therefore, by minimizing  $C_{total}$ , the optimal values of M and N can be obtained. Using (26) and information about the converter power, failure rate, availability and efficiency of the system without redundant branches, which are presented in previous sections, the diagram of Fig. 6 which shows total cost variations in terms of M and N can be obtained.

According to Fig. 6, the minimum cost for the parallel system when  $M = 2$  and  $N = 1$ , is  $C_{total} = 3028.3\$$ . Also, the minimum cost for the standby system when  $M = 2$  and  $N = 1$ , is  $C_{total} = 3049.5\$$ .



(a)



(b)

**Fig. 6.** The converter total cost diagram with N redundant branches in terms of M and N variations; (a) parallel redundant; (b) standby redundant

## 7. CONCLUSION

In this study, reliability calculation of the single-input bidirectional buck-boost dc/dc converter without redundant branches is investigated. Then, this calculation is carried out for the multi-input converter with M main and N redundant branches for both parallel and standby modes and corresponded diagrams are derived. The simulation and calculation results indicated that an increasing number of main branches makes the converter less reliable and available. On the contrary, adding more number of redundant branches causes a decrease in the failure rate and an increase in availability. If the optimization is investigated only in terms of the availability factor, a 100% availability can be achieved with one redundant parallel or standby branch. On the other hand, in terms of failure rate, after adding the sixth redundant parallel branch, the failure rate does not change a lot. This means that adding seventh, eighth, ninth and further redundant branches just increase system cost and complexity. In standby mode, also after adding eighth redundant branch, the increase in the number of redundant branches causes no change in the failure rate. Next, to complete investigations and get the optimal number of branches, the cost calculation is employed and the parametric number of the main and redundant branches of the system is obtained. Through minimizing this function, when the converter has two main branches and one

redundant branch in both modes, the converter is cost effective. Thus, in terms of three factors, i.e. failure rate, availability, and cost, different number of optimal branches can be obtained, which determining the final number of branches depends on the consumer's priorities.

## 8. NOMENCLATURE

$\lambda_{MOSFET}$	Failure rate of power MOSFET (failure/million hours)
$\lambda_{Diode}$	Failure rate of Diode (failure/million hours)
$\lambda_{Inductor}$	Failure rate of Inductor (failure/million hours)
$\lambda_{capacitor}$	Failure rate of Capacitor (failure/million hours)
$\lambda_{OB}$	Base failure rate, operating
$\lambda_{EB}$	Base failure rate, environmental
$\lambda_{TCB}$	Failure rate multiplier, cycling rate
$\lambda_{SJB}$	Base failure rate, solder joint
$\lambda_{IND}$	Failure rate, electrical overstress
$\pi_G$	Reliability growth failure rate multiplier
$\pi_{DCO}$	Failure rate multiplier for duty cycle, operating
$\pi_{TO}$	Failure rate multiplier for temperature, operating
$\pi_S$	Failure rate multiplier for stress
$\pi_C$	Capacitor failure rate multiplier
$\pi_{DCN}$	Failure rate multiplier, duty cycle – non-operating
$\pi_{TE}$	Failure rate multiplier, temperature – environment
$\pi_{CR}$	Failure rate multiplier, cycling rate
$\pi_{DT}$	Failure rate multiplier, delta temperature
$\pi_{SIDT}$	Failure rate multiplier, solder joint delta temperature
$DC$	Duty cycle
$CR$	Cycling rate
$Ea_{op}$	Activation energy, operating
$T_{AO}$	Ambient temperature, operating (in degrees C)
$T_R$	Junction temperature rise above the ambient operating temperature (in degrees C)
$Ea_{nonop}$	Activation energy, non-operating

$T_{AE}$	Ambient temperature, non-operating (in degrees C)
$P_D$	Average power dissipation in a Switching period (W)
$R_{DS}$	Drain –Source on-state resistance of the switch ( $\Omega$ )
$i_s(t)$	Instantaneous switch current (A)
$V_T$	On-state Drain –Source Voltage of the switch (Volts)
$r_D$	On-state resistance of the diode
$i_D(t)$	Instantaneous diode current (A)
$V_F$	Forward voltage of the diode
$r_{esr}$	Internal resistance of the inductor
$i_L(t)$	Instantaneous inductor current (A)
$C_{install}$	Installation cost
$C_{O\&M,s}$	Scheduled operational maintenance cost
$C_{O\&M,u}$	Unscheduled operational maintenance cost
$C_{down}$	Downtime cost
$C_{loss}$	Power loss cost
$\beta$	Function of capacitor type
$Y$	Year of manufacture
MTBF	Mean time before failure
MTTR	Mean time to repair and system is shut-down during that time
$\mu$	Repair rate
A	Availability

## REFERENCES

- [1] Tao H, Kotsopoulos A, Duarte J L, Hendrix M A M., "Family of Multiport Bidirectional DC-DC Converters," *In: IEE Proc.-Electr. Power Appl* 2006; 153: 451-458.
- [2] Song Y, Wang B., "Survey on Reliability of Power Electronic Systems," *IEEE Trans. Power electron*; Vol. 28, pp. 591-604, 2013.
- [3] Yang S, Bryant A, Mawby P, Xiang D, Ran L, Tavner P., "An Industry-Based Survey of Reliability in Power Electronic Converters," *IEEE Trans. Ind. Appl*; Vol. 47, pp. 1441-1451, 2011.
- [4] Behjati H, Davoudi A., "Reliability Analysis Framework for Structural Redundancy in Power Semiconductors," *IEEE Trans. Ind. Electron*; Vol. 60, pp. 4376-4386, 2013.
- [5] Wang H, Blaabjerg F., "Reliability of Capacitors for DC-Link Applications in Power Electronic Converters – An Overview," *IEEE Trans. Ind. Appl*; Vol. 50, pp. 3569-3578, 2014.
- [6] Richardeau F, Pham T T L., "Reliability Calculation of Multilevel Converters: Theory and Applications," *IEEE Trans. Ind. Electron*; Vol. 60, pp. 4225-4233, 2013.



- [7] Nozadian M H B, Zarbil M SH, Abapour M., “**The Effect of Series and Shunt Redundancy on Power Semiconductor Reliability,**” *Journal Power Electron*; Vol. 16, pp. 1426-1437, 2016.
- [8] Kjaer S B, Pedersen J K, Blaabjerg F., “**A Review Of Single-Phase Grid-Connected Inverters for Photovoltaic Modules,**” *IEEE Trans. Ind. Appl*; Vol. 41, pp. 1292–1306, 2005.
- [9] Khwan-on S, Lillo L de, Empringham L, Wheeler P., “**Fault-Tolerant Matrix Converter Motor Drives With Fault Detection of Open Switch Faults,**” *IEEE Trans. Ind. Electron*; Vol. 59, pp. 257–268, 2012.
- [10] Aghdam F H, Abapour M., “**Reliability and Cost Analysis of Multistage Boost Converters Connected to PV Panels,**” *IEEE Journal Photov*; Vol. 6, pp. 981–989, 2016.
- [11] Lezana P, Pou J, Meynard T, Rodriguez J, Ceballos S, Richardeau F., “**Survey on Fault Operation on Multilevel Inverters,**” *IEEE Trans. Ind. Electron*; Vol. 57, pp. 2207–2218, 2010.
- [12] Villani M, Tursini M, Fabri G, Castellini L., “**High Reliability Permanent Magnet Brushless Motor Drive for Aircraft Application,**” *IEEE Trans. Ind. Electron*, Vol. 59, pp. 2073-2081, 2012.
- [13] Khosroshahi A, Abapour M, Sabahi M., “**Reliability Evaluation of Conventional and Interleaved DC-DC Boost Converters,**” *IEEE Trans. Power Electron*, Vol. 30, pp. 5821-5828, 2015.
- [14] Pham T T L, Richardeau F, Gateau G., “**Diagnosis Strategies and Reconfiguration of A 5-Level Double-Boost PFC with Fault-Tolerant Capability,**” *In: IEEE International Symposium on Industrial Electronics (ISIE)*; June 2011; New York, NY, USA: pp. 1857–1862.
- [15] Ceballos S, Pou J, Zaragoza J, Robles E, Villate J L, Martin J L., “**Fault-Tolerant Neutral-Point-Clamped Converter Solutions based On Including A Fourth Resonant Leg,**” *IEEE Trans. Ind. Electron*; Vol. 58, pp. 2293–2303, 2011.
- [16] Pham T T L, Richardeau F, Gateau G., “**Fault Diagnosis and PDPWM Reconfiguration of a 5-level Double-boost PFC with Fault-tolerant Capability,**” *In: Conference on IEEE Industrial Electronics Society. (IECON)*, Nov. 2010, New York, NY, USA: IEEE. pp. 2839–2844.
- [17] Ristow A, Begovic M, Pregelj A, Rohatgi A., “**Development of a methodology for improving photovoltaic inverter reliability,**” *IEEE Trans. Ind. Electron*; Vol. 55, pp. 2581–2592, 2008.
- [18] Denson, W., “**Handbook of 217Plus™ Reliability Prediction Models,**” Utica, NY, USA: RIAC, 2006.
- [19] Yu X, Khambadkone A M., “**Reliability Analysis and Cost Optimization of Parallel-Inverter system,**” *IEEE Trans. Ind. Electron*; Vol. 59, pp. 3881-3889, 2012.